Supramolecular Nanostructures from Side Chain Rod−Coil Polymer Self-Assembly

Byoung-Ki Cho,[†] Moon-Gun Choi,[†] Wang-Cheol Zin,[‡] and Myongsoo Lee*,[†]

Department of Chemistry, Yonsei University, Shinchon 134, Seoul 120-749, Korea, and Department of Materials Science and Engineering, Pohang University of Science and Technology, Pohang 790-784, Korea
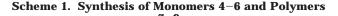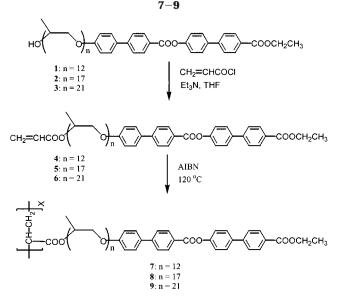
Introduction

Manipulation of supramolecular structure with nanoscale dimensions is of great importance to acquire desired properties for molecular materials, which has potential applications as diverse as membranes, porous materials, nanoreactors, and nanowires. Various molecular engineering in shape and size has been performed to control supramolecular structure which determines physical properties of molecular materials.[1−6] Previously, we have explored a strategy to control supramolecular architecture: adopting rod−coil molecules which consist of a rigid aromatic rod block and a flexible aliphatic coil block. Recent observations from our laboratory have shown that rod−coil molecules self-organize into various supramolecular architectures such as lamellar, 3-D honeycomb, bicontinuous cubic, hexagonal columnar, and body-centered tetragonal structures depending on diverse molecular parameters.[7] In addition, we have shown that the rod−coil approach as a means to control supramolecular structure could be extended to main-chain rod−coil multiblock copolymer systems which generate bicontinuous cubic and hexagonal columnar phase depending on rod-to-coil volume fraction.[8] Recently, we have also demonstrated that systematic variation of the number of repeating units in a rod−coil multiblock copolymeric system can regulate the shape and size of the supramolecular architecture formed by self-assembly of the rod segments.[9]

A novel strategy to manipulate the supramolecular structure can also be accessed by converting rod−coil monomer into side chain polymer. Contrary to the monomer, the coil termini in the side chain polymer are stitched into a polymer backbone through covalent linkage; thus, selective shrinkage of the coil domains in the microphase-separated supramolecular structure self-assembled by rod−coil monomers would take place upon polymerization. Consequently, simple polymerization of rod−coil monomer could frustrate the formation of supramolecular structure with large interfacial area relative to that of the rod−coil monomer. This suggests that the control of self-assembled supramolecular structure in the rod−coil system is possible by stitching the polymerizable group at the coil termini of rod−coil molecules through polymerization. With this in mind, we have synthesized a series of rod−coil monomers **4**−**6** and their corresponding polymers **7**−**9** consisting of a rigid rod made up of two biphenyls

[†] Yonsei University.
[‡] Pohang University of Science and Technology.
* To whom correspondence should be addressed. Fax 82-2-364-7050; e-mail mslee@yonsei.ac.kr.

Scheme 1. Synthesis of Monomers 4−6 and Polymers 7−9

connected through ester linkages and flexible poly(propylene oxide) (PPO) coils with different lengths. Since the monomer and corresponding polymer have an identical constituting unit of PPO chain, the supramolecular structural behavior of liquid crystalline state can only be attributed to the stitching of the coil termini by polymerization. We report herein the results on supramolecular structural behavior in the melt state upon polymerization of the rod−coil monomers.

Experimental Section

Synthesis. A general outline of the synthetic procedure is shown in Scheme 1.

Synthesis of Ethyl 4-[4-[Oxypoly(propyleneoxy)propyloxy]-4′-biphenylcarboxyloxy]-4′-biphenyl Carboxylates (1−3). Ethyl 4-[4-[oxypoly(propyleneoxy)propyloxy]-4′-biphenylcarboxyloxy]-4′-biphenyl carboxylates (**1**−**3**) were all synthesized using the reported procedure.[7a]

Synthesis of Monomers 4−6. All of the monomers **4**−**6** were synthesized using the same procedure. A representative example is described for **4**. Compound **4** (0.29 g, 0.25 mmol) and triethylamine (0.11 mL, 0.77 mmol) were dissolved in 20 mL of tetrahydrofuran. Acryloyl chloride (0.04 mL, 0.44 mmol) was added dropwise to the mixture via a syringe. The solution was stirred at room temperature under nitrogen overnight. After the solvent was removed in a rotary evaporator, the mixture was extracted with methylene chloride and aqueous 1 N HCl solution. The methylene chloride fraction was washed with water, dried over anhydrous magnesium sulfate, and filtered. After removing the solvent, the crude product was purified by column chromatography (silica gel) sequentially from methylene chloride−ethyl acetate (4:1) to ethyl acetate eluents to yield 0.25 g (84%) of a white solid. ^{1}H NMR (250 MHz, CDCl$_3$, δ, ppm): 8.24 (d, 2Ar−H, *o* to COOphenyl, $J = 7.8$ Hz), 8.12 (d, 2Ar−H, *o* to COOCH$_2$, $J = 7.7$ Hz), 7.65−7.71 (m, 6Ar−H, *m* to COOphenyl, *m* to biphenylcarboxylate and *m* to COOCH$_2$), 7.59 (d, 2Ar−H, *m* to CH(CH$_3$)O, $J = 8.5$ Hz), 7.35 (d, 2Ar−H, *o* to biphenylcarboxylate, $J = 8.5$ Hz), 7.04 (d, 2Ar−H, *o* to CH(CH$_3$)O, $J = 8.6$ Hz), 6.39 (dd, 1H, C*H*$_2$=CH, $J = 17.4$ and 1.5 Hz), 6.11 (dd, 1H, CH$_2$=C*H*, $J = 17.4$ and 10.2 Hz), 5.78 (dd, 1H, C*H*$_2$=CH, $J = 10.2$, 1.5 Hz), 5.09 (m, CH$_2$=CHCOOC*H*$_2$ or CH$_2$=CHCOOC*H*(CH$_3$)), 4.58 (m, CH$_2$C*H*(CH$_3$)Ophenyl or (CH$_3$)CHC*H*$_2$Ophenyl), 4.41 (q, 2H, OC*H*$_2$CH$_3$, $J = 7.1$ Hz), 3.15−3.91 (m, OC*H*$_2$C*H*(CH$_3$)),

Table 1. Thermal Transitions of Monomers 4−6 and Polymers 7−9 (Data Are from Second Heating and First Cooling Scans)[a]

compound	$\bar{M}_w/\bar{M}_n$[b]	M_n (GPC)	phase transitions (°C) and corresponding enthalpy changes (kJ/mol)	
			heating	cooling
4	1.04		k 39.1 (16.6) cub 62.1 (1.0) i	i 53.1 (1.0) cub
5	1.04		k 26.8 (2.0) col 49.8 (0.8) i	i 40.8 (0.7) col 22.0 (1.7) k
6	1.04		k 25.9 (1.9) col 41.4 (0.8) i	i 33.5 (0.7) col 21.0 (1.4) k
7	2.80	118 600	k 46.2 (2.1) cub 151.2 (1.9) i	i 138.8 (1.5) cub
8	2.37	63 100	k 41.0 (0.6) cub 103.3 (0.7) col 109.7 (0.7) i	i 96.4 (0.4) col 89.2 (0.3) cub 29.8 (0.6) k
9	2.75	134 500	k 39.1 (1.6) col 97.1 (0.9) i	i 86.0 (0.7) col 30.9 (1.4) k

[a] k = crystalline, cub = bicontinuous cubic, col = hexagonal columnar, i = isotropic. [b] Determined from GPC data.

1.34−1.45 (m, 6H, CH₂C*H₃* and C*H*(C*H₃*)Ophenyl), 0.90−1.30 (m, 33H, OCH₂CH(C*H₃*)); $\bar{M}_w/\bar{M}_n$ = 1.04 (GPC). Anal. Calcd for C₆₇H₉₆O₁₈: C, 67.65; H, 8.13. Found: C, 67.65; H, 8.13.

5: yield 80%. ¹H NMR (250 MHz, CDCl₃, δ, ppm): 8.24 (d, 2Ar−H, *o* to COOphenyl, *J* = 7.8 Hz), 8.12 (d, 2Ar−H, *o* to COOCH₂, *J* = 7.7 Hz), 7.65−7.71 (m, 6Ar−H, *m* to COOphenyl, *m* to biphenylcarboxylate and *m* to COOCH₂), 7.59 (d, 2Ar−H, *m* to CH(CH₃)O, *J* = 8.5 Hz), 7.35 (d, 2Ar−H, *o* to biphenylcarboxylate, *J* = 8.5 Hz), 7.04 (d, 2Ar−H, *o* to CH-(CH₃)O, *J* = 8.6 Hz), 6.39 (dd, 1H, C*H₂*=CH, *J* = 17.4 and 1.5 Hz), 6.11 (dd, 1H, CH₂=C*H*, *J* = 17.4 and 10.2 Hz), 5.78 (dd, 1H, C*H₂*=CH, *J* = 10.2, 1.5 Hz), 5.09 (m, CH₂=CHCOOC*H₂* or CH₂=CHCOOC*H*(CH₃)), 4.58 (m, CH₂C*H₃*)Ophenyl or (CH₃)CHC*H₂*Ophenyl), 4.41 (q, 2H, OC*H₂*CH₃, *J* = 7.1 Hz), 3.14−3.91 (m, OC*H₂*C*H*(CH₃)), 1.35−1.44 (m, 6H, CH₂C*H₃* and C*H*(C*H₃*)Ophenyl), 0.85−1.34 (m, 48H, OCH₂CH(C*H₃*)); $\bar{M}_w/\bar{M}_n$ = 1.04 (GPC). Anal. Calcd for C₈₂H₁₂₆O₂₃: C, 66.55; H, 8.58. Found: C, 66.47; H, 8.84.

6: yield 78%. ¹H NMR (250 MHz, CDCl₃, δ, ppm): 8.24 (d, 2Ar−H, *o* to COOphenyl, *J* = 7.8 Hz), 8.12 (d, 2Ar−H, *o* to COOCH₂, *J* = 7.7 Hz), 7.65−7.72 (m, 6Ar−H, *m* to COOphenyl, *m* to biphenylcarboxylate and *m* to COOCH₂), 7.60 (d, 2Ar−H, *m* to CH(CH₃)O, *J* = 8.5 Hz), 7.35 (d, 2Ar−H, *o* to biphenylcarboxylate, *J* = 8.5 Hz), 7.04 (d, 2Ar−H, *o* to CH-(CH₃)O, *J* = 8.6 Hz), 6.39 (dd, 1H, C*H₂*=CH, *J* = 17.4 and 1.5 Hz), 6.11 (dd, 1H, CH₂=C*H*, *J* = 17.4 and 10.2 Hz), 5.78 (dd, 1H, C*H₂*=CH, *J* = 10.2, 1.5 Hz), 5.09 (m, CH₂=CHCOOC*H₂* or CH₂=CHCOOC*H*(CH₃)), 4.58 (m, CH₂C*H*(CH₃)Ophenyl or (CH₃)CHC*H₂*Ophenyl), 4.40 (q, 2H, OC*H₂*CH₃, *J* = 7.1 Hz), 3.15−3.91 (m, OC*H₂*C*H*(CH₃)), 1.35−1.44 (m, 6H, CH₂C*H₃* and CH(C*H₃*)Ophenyl), 0.85−1.35 (m, 60H, OCH₂CH(C*H₃*)); $\bar{M}_w/\bar{M}_n$ = 1.04 (GPC). Anal. Calcd for C₉₄H₁₅₀O₂₇: C, 65.94; H, 8.83. Found: C, 65.95; H, 9.08.

Synthesis of Polymers 7−9. All of the polymers **7−9** were synthesized using the same procedure. A representative example is described for **7**. Monomer **4** (0.20 g) and 0.5 wt % azobis(isobutyronitrile) (AIBN, 1 mg) were dissolved in methylene chloride. The solvent was subsequently removed under vacuum. Polymerization was carried out in a two-neck flask under vacuum at 120 °C for 12 h without solvent. The resulting polymers were purified by precipitation from methylene chloride solution into methanol and were collected by filtration. The filtered polymers were dried and reprecipitated from methylene chloride solution into methanol until GPC curve showed no traces of oligomers.

Results and Discussion

The synthesis of monomers and corresponding polymers is outlined in Scheme 1. Ethyl 4-[4-[oxypoly-(propyleneoxy)propyloxy]-4′-biphenylcarboxyloxy]-4′-biphenyl carboxylates (**1−3**) were all synthesized using the reported procedure.[7a] The monomers **4−6** were prepared from the reaction of corresponding precursor molecules **1−3** with acryloyl chloride in the presence of triethylamine. The resulting monomers were purified by column chromatography (silica gel) sequentially from methylene chloride−ethyl acetate (4:1) to ethyl acetate eluents until the polydispersity values remained constant. All analytical data of monomers were consistent
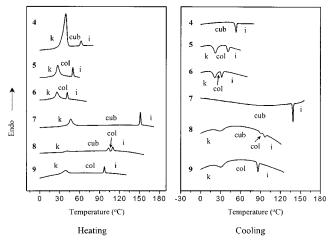

Figure 1. DSC traces (10 °C min⁻¹) recorded during the heating and cooling scans of monomers **4−6** and polymers **7−9**.

with expected molecular structures. Molecular weight distributions of these monomers determined from GPC appeared to be less than 1.04 as shown in Table 1, indicative of high purity. The resulting monomers were polymerized through bulk polymerization at 120 °C for 12 h in the presence of AIBN initiator. The obtained polymers were then purified by several reprecipitation from methylene chloride solution into methanol. The number-average molecular weights and the molecular weight distributions of the polymers determined by GPC appeared to be in the range 60 000−130 000 g/mol and 2.3−2.8, respectively, with reference to polystyrene standards (Table 1).

The thermal transition temperatures and the nature of the mesophase were investigated by DSC and thermal polarized optical microscopy as summarized in Table 1. Figure 1 shows the DSC heating and cooling scans of the monomers and the corresponding polymers. As shown in Figure 1, all of the monomers and polymers exhibit thermotropic liquid crystalline phases. Monomer **4** with short length of PPO coil (DP = 12) exhibits a crystalline melting transition at 39 °C, followed by a mesophase that undergoes isotropization at 62 °C, whereas the corresponding polymer **7** shows a crystalline melting transition at 46 °C and a transition from mesophase to isotropic liquid at 151 °C. As expected,[10,11] temperature range and thermal stability of the mesophase increase upon polymerization. On the polarized optical microscope, no birefringence between cross polarizers after the melting of both **4** and **7** could be observed, suggesting the existence of an optically isotropic cubic mesophase.[7,8,12,13] To investigate the microstructure of this mesophase, X-ray scattering experiments have been performed. The sharp small-angle X-ray reflections at the relative position ratios of √6, √8, √22, and √26 could be observed from **4** at 60 °C.
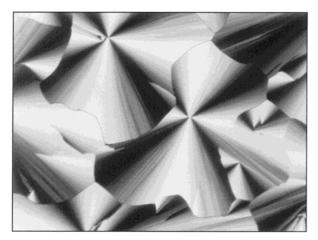
Figure 2. Representative optical micrograph (100×) of texture exhibited by hexagonal columnar mesophase of **5** at 38 °C on a cooling scan.

Table 2. Characterization of Monomers 4−6 and Polymers 7−9 by Small-Angle X-ray Scattering in the Liquid Crystalline Phase

| compd | cubic | | columnar | |
	d_{211} (Å)	lattice constant (*a*) (Å)	d_{100} (Å)	lattice constant (*a*) (Å)
4	53.8	131.8		
5			58.9	68.0
6			60.9	70.3
7	54.6	133.8		
8	61.4	150.4	59.1	68.3
9			64.4	74.4

The positions of these reflections can be indexed as the 211, 220, 332, and 431 reflections of *Ia3d* symmetry, similar to the results reported previously from our and other laboratories.[7,8,14] From the observed *d* spacing of 211 reflections, the best fit value for the bicontinuous cubic lattice constant of **4** is 131.8 Å (Table 2). Polymer **7** also exhibits similar diffraction patterns in the liquid crystalline phase, indicative of a bicontinuous cubic mesophase with a lattice constant of 133.8 Å. WAXS patterns of both **4** and **7** display only a diffuse halo at their mesomorphic temperatures, as evidence of the lack of any positional long-range order other than the three-dimensional cubic packing.

Monomer **5** with intermediate length of coil (DP = 12) exhibits a crystalline melting transition at 27 °C, followed by a columnar mesophase which, in turn, undergoes transformation into isotropic liquid at 50 °C. The optical microscopic observation of **5** is consistent with this behavior. On cooling from isotropic liquid of **5**, first a spherulitic growing of texture can be observed with a final development of pseudo-focal conic domains which are characteristic of a hexagonal columnar mesophase exhibited by other rod−coil molecules illustrated in previous publication (Figure 2).[7,8] The SAXS pattern in the melt state recorded at 40 °C displays three peaks with the *d*-spacing ratio of 1:$\sqrt{3}$:$\sqrt{4}$, which can be interpreted as a hexagonal columnar structure with a lattice constant *a* = 68.0 Å (Table 2). Only a diffuse halo can be observed in the WAXS pattern. In contrast to monomer **5**, the corresponding polymer **8** exhibits an endothermic peak at 103 °C on DSC heating scan, in addition to the crystal melting and isotropic liquid transitions at 41 and 110 °C, respectively (Figure 1). From the observation of polarized optical microscopy, isotropic rectangular and rhombic areas with straight
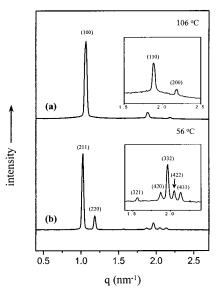

Figure 3. Small-angle X-ray diffraction patterns measured at different temperatures plotted against *q* (= $4\pi \sin \theta/\lambda$) in (a) the hexagonal columnar mesophase at 106 °C and (b) the bicontinuous cubic mesophase at 56 °C for **8**.

edges could be observed on the pseudo-focal conic domains on cooling, suggesting that the additional endothermic peak of the polymer corresponds to a cubic−columnar mesomorphic transition.[7a,b] As shown in Figure 3a, the SAXS pattern measured at the higher temperature mesophase (106 °C) of the polymer shows three sharp peaks similar to those of the monomer, corresponding to a hexagonal columnar structure with a lattice constant *a* = 68.3 Å. In contrast to that of the monomer, the SAXS pattern in the lower temperature mesophase (56 °C) of the polymer displays a number of reflections, corresponding to a bicontinuous cubic structure with a lattice constant *a* = 150.4 Å (Figure 3b). At wide angle, only diffuse halo could be observed in the temperature range of both mesophases, indicating that there are only weak liquidlike arrangements of the rod segments within the aromatic domains.

On the basis of these observations, we can conclude that polymer **8** displays a bicontinuous cubic phase in addition to a hexagonal columnar phase. These results demonstrate that polymerization of rod−coil monomer into side chain polymer can give rise to large structural transformation from 2-D hexagonal to 3-D cubic structures, as illustrated schematically in Figure 4. This unique phase behavior can be speculated by considering variation in the specific volume of coil segments upon polymerization. Selective stitching of the coil segments through polymerization of acryl groups at the coil termini would decrease the space occupied by coil segments in the microphase-separated supramolecular structure, while that of the rod domains remained essentially constant. Consequently, the hexagonal columnar structure of the monomer would be unstable upon polymerization, giving rise to a bicontinuous cubic structure that allows less volume for coils. Another factor that could play a role in transformation from 2-D hexagonal to 3-D cubic structures is the decrease in entropy upon polymerization, giving rise to the structure with smaller interfacial area. Therefore, polymerization of rod−coil monomer produces an effect similar to varying the rod to coil volume ratio.[7,8,15]

In the case of monomer **6** and its corresponding polymer **9** based on long length of poly(propylene oxide)
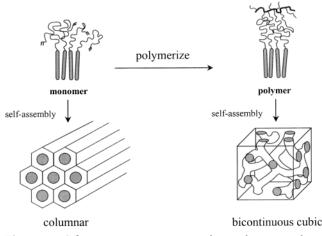
Figure 4. Schematic representation of transformation from hexagonal columnar to bicontinuous cubic structures through polymerization.

coil (DP = 12), only a hexagonal columnar mesophase is exhibited after crystalline melting. SAXS patterns of both molecules display three sharp X-ray reflections, corresponding to a hexagonal columnar structure with lattice constants $a = 70.3$ and 74.4 Å, respectively; only a diffuse halo could be observed in the wide-angle range, indicative of liquidlike arrangement of the rods within the domains.

The tendency to transform from a columnar into a bicontinuous cubic structure by decreasing coil volume fraction is consistent with the results reported previously from our laboratory.[7a,b,8,15] However, it is remarkable that this structural transformation is also accompanied by simple polymerization of rod−coil monomer containing acryl group at the coil terminus. Polymerization of acryl group stitches coil segments into a polymer backbone produces selective shrinkage of coil domains in the microphase-separated supramolecular structure. This is likely to be responsible for the transformation of the hexagonal columnar structure exhibited by the monomer into a bicontinuous cubic structure that allows less volume for coil upon polymerization.

Supporting Information Available: Small-angle X-ray diffraction patterns of monomers **4**−**6** and polymers **7** and **9**; wide-angle X-ray diffraction patterns of monomers **4**−**6** and polymers **7**−**9**. This material is available free of charge via the Internet at http://pubs.acs.org.

References and Notes

(1) Muthukumar, M.; Ober, C. K.; Thomas, E. L. *Science* **1997**, *277*, 1225.
(2) Lee, M.; Cho, B.-K.; Zin, W.-C. *Chem. Rev.* **2001**, *101*, 3869.
(3) Jenekhe, S. A.; Chen, X. L. *Science* **1998**, *279*, 1903.
(4) Widawski, G.; Rawiso, M.; Francois, B. *Nature (London)* **1994**, *369*, 387.
(5) Stupp, S. I.; LeBonheur, V.; Walker, K.; Li, L. S.; Huggins, K. E.; Keser, M.; Amstutz, A. *Science* **1997**, *276*, 384.
(6) Percec, V.; Ahn, C.-H.; Ungar, G.; Yeardley, D. J. P.; Möller, M.; Seiko, S. S. *Nature (London)* **1998**, *391*, 161.
(7) (a) Lee, M.; Cho, B.-K.; Kim, H.; Yoon, J.-Y.; Zin, W.-C. *J. Am. Chem. Soc.* **1998**, *120*, 9168. (b) Lee, M.; Cho, B.-K.; Kim, H.; Zin, W.-C. *Angew. Chem., Int. Ed. Engl.* **1998**, *37*, 638. (c) Lee, M.; Cho, B.-K.; Jang, Y.-G.; Zin, W.-C. *J. Am. Chem. Soc.* **2000**, *122*, 7449. (d) Lee, M.; Oh, N.-K.; Zin, W.-C. *Chem. Commun.* **1996**, 1787. (e) Lee, M.; Cho, B.-K.; Ihn, K. J.; Lee, W.-K.; Oh, N.-K.; Zin, W.-C. *J. Am. Chem. Soc.* **2001**, *123*, 4647. (f) Cho, B.-K.; Lee, M.; Oh, N.-K.; Zin, W.-C. *J. Am. Chem. Soc.* **2001**, *123*, 9677.
(8) (a) Lee, M.; Cho, B.-K.; Kang, Y.-S.; Zin, W.-C. *Macromolecules* **1999**, *32*, 7688. (b) Lee, M.; Cho, B.-K.; Kang, Y.-S.; Zin, W.-C. *Macromolecules* **1999**, *32*, 8531.
(9) Lee, M.; Cho, B.-K.; Oh, N.-K.; Zin, W.-C. *Macromolecules* **2001**, *34*, 1987.
(10) Percec, V.; Keller, A. *Macromolecules* **1990**, *23*, 4347.
(11) (a) Pugh, C.; Kiste, A. L. In *Handbook of Liquid Crystals*; Demus, D., Goodby, J., Grey, G. W., Spiess, H.-W., Vill, V., Eds.; Wiley-VCH: Weinheim, 1998; Vol. 3, pp 152−156. (b) Percec, V.; Lee, M. *Macromolecules* **1991**, *24*, 1017. (c) Lee, M.; Park, K.-S. *Polym. Bull. (Berlin)* **1997**, *39*, 149.
(12) (a) Demus, D.; Richter, L. *Textures of Liquid Crystals*; Verlag Chemie: Weinheim, 1978. (b) Gray, G. W.; Goodby, J. W. *Smectic Liquid Crystals. Textures and Structures*; Leonard Hill: Glasgow, 1984.
(13) Stauffer, G.; Schellhorn, M.; Lattermann, G. *Liq. Cryst.* **1995**, *18*, 519.
(14) (a) Luzzati, V.; Spegt, P. A. *Nature (London)* **1967**, *215*, 701. (b) Rancon, Y.; Charvolin, J. *J. Phys. Chem.* **1988**, *92*, 2646. (c) Clerc, M.; Levelut, A. M.; Sadoc, J. F. *J. Phys. II* **1991**, *1*, 1263. (d) Sakurai, S.; Irie, H.; Umeda, H.; Nomura, S.; Lee, H.; Kim, J. K. *Macromolecules* **1998**, *31*, 336.
(15) Lee, M.; Oh, N.-K.; Lee, H.-K.; Zin, W.-C. *Macromolecules* **1996**, *29*, 5567. (b) Lee, M.; Cho, B.-K. *Chem. Mater.* **1998**, *10*, 1894. (c) Lee, M.; Jang, D.-W.; Kang, Y.-S.; Zin, W.-C. *Adv. Mater.* **1999**, *11*, 1018.

MA011676X